

## A DIDACTICAL PERSPECTIVE ON THE APPLICATION OF THE MAGNETO-OPTIC KERR EFFECT IN VERSATILE STUDIES OF MODERN MAGNETIC MATERIALS

C. KUNCSEER, A. KUNCSEER and S. ANTOHE

University of Bucharest, Faculty of Physics, Atomistilor Street 405, P.O. Box MG-11,  
Măgurele-Ilfov, 077125, Romania  
E-mail: ckuncser@yahoo.com

*Received July 19, 2011*

*Abstract.* Devices based on the magneto-optical Kerr effect are versatile and powerful tools for the magnetic characterization of thin films and multilayers. The magneto optic effects are introduced by starting from a simple pictorial phenomenology. The microscopic origin is also mentioned as well as a brief description of the macroscopic formalism. The main advantages of the MOKE magnetometry as compared to conventional magnetometry are briefly discussed together with different experimental configurations. Finally, the working principles and a detailed explanation of a Faraday cell based MOKE magnetometer is presented. The performances and the capabilities of the mentioned device are exemplified in case of magnetic thin films with transition metals.

*Key words:* physics education, MOKE magnetometry, magnetic thin films.

### 1. INTRODUCTION

The development of advanced magnetic nanomaterials, with a significant technological impact in our days, was related both to the refinement of the synthesis and processing methods as well as to the improved or newly discovered investigation tools. Many efforts have been devoted to the characterization of the nanosized layered systems as thin films and exchange coupled multilayers, presenting interesting magnetic phenomena like as exchange spring [1, 2] and exchange bias [2, 3], with direct applications in nanoelectronics [4, 5]. High-density information storage media [6] are other types of structures of large interest with respect to their magnetic characterization. Accordingly, of particular interest in magnetically anisotropic systems is the understanding of the magnetization reversal process. The most usual experimental approach providing the magnetization reversal is to follow the magnetization of the sample,  $M$ , while cycling the applied magnetic field, with the result of the so called magnetic hysteresis loop. Common techniques to measure the magnetic hysteresis loop of

layered systems are magnetometry techniques [7] based on the detection of sample induced flux variations (*e.g.* vibrating sample magnetometry (VSM) or superconducting quantum interference device (SQUID) magnetometry), but microscopic element selective techniques providing the in-field reorientation of the magnetic moments (spins) of given elements are also available (*e.g.* in-field Conversion Electron Mossbauer Spectroscopy [8]). However a versatile and powerful tool to measure the magnetization reversal in thin films and multilayers is the magneto-optic Kerr effect (MOKE) magnetometry, which employs the dependence of the characteristics of the light reflected on the sample surface (intensity and phase), on the sample magnetization. Due to its high sensitivity to the magnetization within the skin depth region of metallic materials (10-20 nm), the effect is mainly useful in the study of surface magnetism. It can also probe the magnetization in very small regions of materials (wires, patterns, dots) or even in real micro-devices for applications. Further on, the present commercially available magneto-optic drivers are also based on the Kerr effect. In spite of a simple principle at a first view, the microscopic origin of the effect as well as its macroscopic formalism is not trivial (especially when applied to the multilayer case). This paper deals with a didactical presentation of the effect, which is introduced in a pictorial-like fashion, in order to understand the terminologies and the working principle of a real experimental device. The performances and the capabilities of the mentioned device are exemplified in case of magnetic thin films with transition metals. The main advantages of the MOKE magnetometry as compared to conventional magnetometry are also discussed, together with the modern educational procedures assuring the better understanding of such complex physical processes the mainly goals of research in physics education [9, 10].

## 2. A PICTORIAL PRESENTATION OF MAGNETO OPTIC PHENOMENA

Polarization is one of the most known phenomena supporting the wave character of light. Accordingly, the light is a transverse electromagnetic wave which can be linearly or elliptically/circularly polarized. A linear polarized light is a wave with the electric field vector,  $\mathbf{E}$ , oscillating along a given direction, perpendicular to the propagation direction (sometimes, this kind of polarization is called plane polarization, the plane of polarization being the plane defined by the direction of the electric field and the direction of propagation). In an elliptically polarized light, the electric field rotates during the propagation, describing an ellipse in a plane perpendicular to the propagation direction (when a circle is described, the wave is called circularly polarized). It can be proven that any linearly polarized wave can be seen as a superposition of two circularly polarized components, namely a left-circularly polarized (LCP) and a right-circularly polarized (RCP) one, of amplitudes  $E_L = E_R = E/2$ . On the other hand, an elliptically

polarized light can be seen as a superposition of two linearly polarized components which are out of phase and with different amplitudes (if the electric fields of the two components are equal, the resulting light is circularly polarized).

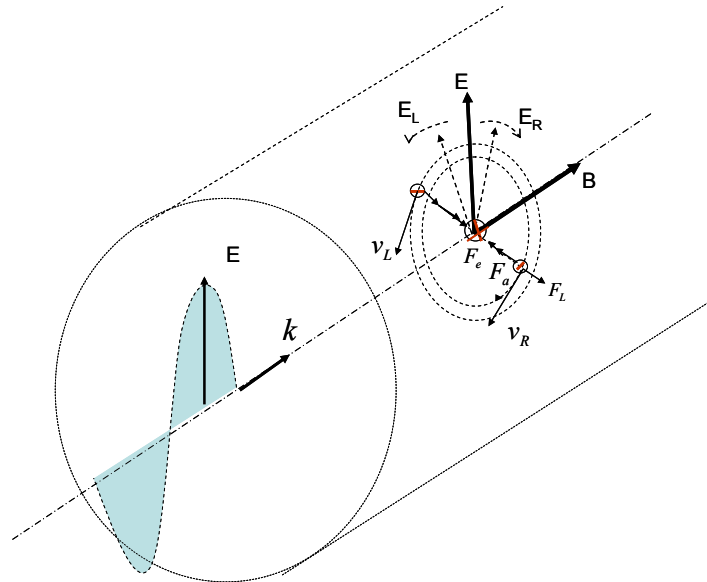


Fig. 1 – A pictorial representation explaining the Faraday effect.

Let's suppose a linearly polarized light passing through a medium formed by free electrons and fixed positive centers, distributed in such a way to fulfill the local condition of charge neutrality. The linearly polarized wave can be seen as a superposition of the two above mentioned circularly polarized components, LCP and RCP (Fig. 1). Obviously, the LCP electric field will drive the electrons into a left circular motion around a fix positive center whereas the RCP electric field will drive the electrons into a right circular motion (alternatively, the oscillations of the electrons under the influence of the linear polarized light can be decomposed into two opposite circular components). The radius of the circular trajectory is established through the equilibrium of the forces acting on the electron, within the assumption that the pair electron-positive center forms a rotating electric dipole with an attractive recovering force (imposed by the neutrality condition),  $\mathbf{F}_a$ , proportional to the radius,  $\mathbf{r}$ , of the circular orbit ( $\mathbf{F}_a = -k\mathbf{r}$ ). In the absence of any applied magnetic field, the radii of both orbits of electrons in left and right circular motion are equal, as given by the equation:

$$eE_{L,R} + kr_{L,R} = m\omega^2 r_{L,R} \Rightarrow r_{L,R} = \frac{eE / 2m}{(\omega^2 - \omega_0^2)}, \quad (1)$$

with  $\omega$ , the angular frequency of the radiation,  $m$ , approaching the electron mass and  $\omega_0^2 = k/m$ , a material dependent constant ( $\omega > \omega_0$ ).  $E$  is the amplitude of the electric field of the wave and  $e$ , the elementary charge. Since the electric dipole moment,  $P_i$ , is proportional to the radius of the circular orbit ( $\mathbf{P}_i = e\mathbf{r}$ ), it results straightforward from  $\mathbf{D} = \varepsilon\mathbf{E} = \varepsilon_0\mathbf{E} + \mathbf{P}$  with  $P = NP_i$  ( $N$ = number of dipoles per unit volume), that the dielectric constant,  $\varepsilon$ , can be expressed as:

$$\varepsilon = \varepsilon_0 \left( 1 + \frac{Ne^2 / 2m\varepsilon_0}{\omega^2 - \omega_0^2} \right). \quad (2)$$

Taking into account that  $n^2 = \varepsilon_r = \varepsilon/\varepsilon_0$  ( $\mu_r = 1$ ), it will be no difference between the dielectric constants and the corresponding refractive indices seen by the left- and right-circularly polarized electromagnetic components. At variance to this situation, if a magnetic field is applied along the propagation direction of the wave, additional Lorentz forces will act differently on electrons with left and right rotating motion, respectively (Fig.1). Hence, the radii of the two circular orbits become different, according to the equations:

$$eE_{L,R} + kr_{L,R} \pm e\omega r_{L,R} B = m\omega^2 r_{L,R} \Rightarrow r_{L,R} = \frac{eE / 2m}{(\omega^2 - \omega_0^2 \mp \omega Be / m)}. \quad (3)$$

Consequently, the dielectric constants and the corresponding refractive indices  $n_L$  and  $n_R$  seen by the left- and right-circularly polarized waves are different, leading to different propagation velocities. Finally, after the light travels a distance  $L$  through the medium, the two circularly polarized waves show a phase difference  $\Delta\theta = (\omega L/c)(n_L - n_R)$ . Summing up the two circularly polarized components at the emergence from the medium, it results a linearly polarized wave which polarization direction is rotated at an angle  $\theta = \Delta\theta/2$  from the initial direction. Based on eqs. (2) and (3), the two refractive indices,  $n_L$  and  $n_R$  can be expressed *via* the relationship:

$$n_{L,R}^2 = 1 + \frac{Ne^2 / 2m\varepsilon_0}{\omega^2 - \omega_0^2 \mp \omega Be / m} \cong n^2 (1 \pm \xi), \quad (4)$$

with :

$$n^2 = 1 + \frac{Ne^2 / 2m\varepsilon_0}{\omega^2 - \omega_0^2} \quad \text{and} \quad \xi = \frac{\omega Be}{m} \frac{1}{\omega^2 - \omega_0^2}. \quad (5), (6)$$

While  $\xi \ll 1$ , equation (4) can be expressed as:

$$n_{L,R} \cong n \left( 1 \pm \frac{1}{2} \xi \right) \quad (7)$$

and the rotation of the polarization plane can be approximated by:

$$\theta = \frac{\omega L}{2c} (n_L - n_C) \cong \frac{\omega L n \xi}{2c} \cong \frac{ne}{2mc} \frac{\omega^2}{\omega^2 - \omega_0^2} LB \cong K(\omega) LB. \quad (8)$$

The above relation obtained *via* a simple phenomenological explanation resumes the essence of the Faraday effect, which observation represented the birth of the magneto-optics (MO). In particular, in 1845, Michael Faraday observed the rotation of the polarization plane of a linearly polarized light propagating through a piece of lead-borosilicate glass placed in magnetic field, whereas John Kerr observed in between 1876–1878 the rotation of the polarization plane of a linearly polarized light upon reflection from the surface of a piece of Fe with either in plane or perpendicular to plane polarization. A conclusive history on the discovery and the continuous progress of magneto-optics was presented in [11]. According to relation (8) the rotation angle  $\theta$  is proportional to the strength of the applied field,  $B$ , and the length,  $L$ , of the pathway along the light propagates through the medium, the proportional constant being dependent on the light wavelength (subsequently, Verdet and Voigt exploited further such a relationship, the proportionality constant being known as the Verdet constant). However, already at the end of the 19<sup>th</sup> century, it was observed that this linear dependence does not hold for ferromagnetic materials, which usually presents also very large MO effects. Earlier attempts to estimate the magnitude of the effective fields which might provide rotation angles close to the observed ones in ferromagnetic materials, led to values of  $10^2$ – $10^3$  T, approaching the value of the Weiss field (introduced later for explaining the origin of the ferromagnetism). Hence, in case of ferromagnetic materials, the field  $B$  in relation (8) has to be replaced by the total field,  $B = B_0(1+\chi)$ , where  $B_0 = \mu_0 H$ , is the magnetic induction in vacuum and  $\chi$  is the magnetic susceptibility ( $\chi = \mu_0 M/B_0$ , with  $M$  the magnetization). While in case of ferromagnetic materials,  $\chi \gg 1$ , it results  $B = B_0 \chi = \mu_0 M$ , and hence, relation (8) shows that in this case the rotation angle is proportional to  $L$  and the magnetization,  $M$ , of the medium. Although relation (8) seems to reproduce the main characteristics of the Faraday effects for any material, two additional aspects have to be mentioned: (i) the refractive index estimated through  $n^2 = \epsilon_r$  is still valid in ferromagnetic materials with significant susceptibilities, while the magnetic relative permeability can be further approximated by 1 at optical frequencies ( $\mu_r(\omega) = 1$ ), and (ii) the effective Weiss field can not explain alone the Faraday effect while it is not coupled to the electron motion which ultimately determines the dielectric properties of the material. It was Hulme in 1932 who pointed out that in fact, microscopically, the spin orbit interaction is the one coupling the magnetic moment of the electron with its motion, which in turn responds also to the electric field of the light, connecting thus the magnetic and optical properties of a ferromagnetic material. However, the basic origin of the magneto-optics was quite well understood at the middle of the 20<sup>th</sup> century and a further significant progress was related especially to a continuous improvement of the experimental techniques and to the macroscopic description related to the general case of magnetic multilayer.

Looking in a greater detail to the phenomenological model expressing the linearly polarized light as a superposition of two circularly polarized components, there are actually two processes taking place for the light propagating through a magnetized medium: (i) the two polarized components travelling with different velocities emerge from the media with different phase shifts, leading to the Faraday rotation and (ii) the two components could present different absorption coefficients, leading to different amplitudes of the emergent electric fields,  $E_L$  and  $E_R$ , and so, to a given ellipticity of the outgoing light. Hence, the refractive indices  $n_{L,R}$  have to be complex parameters and can be expressed by extending eq. (7) to the case of a complex refractive index,  $n^* = n + i\kappa$  and by taking into account that the perturbation,  $\xi$  of the refractive index *via* the magnetic field is not dependent only on the magnitude of  $\mathbf{B}$ , but also on its orientation with respect to the propagation direction,  $\mathbf{u}_k = \mathbf{k}/k$  ( $\mathbf{k}$  is the wave vector in vacuum and  $\mathbf{u}_k$  is its versor). In the general case,  $\xi$  can be written as the product  $\mathbf{Q} \cdot \mathbf{u}_k$ , where  $\mathbf{Q}$  is called the Voight vector and is proportional to the field induction  $\mathbf{B}$  (or magnetization  $\mathbf{M}$ ). It is worth mentioning that in the case with  $\mathbf{B}$  along  $\mathbf{u}_k$ ,  $\xi = Q$  and is proportional to  $B$  according to relation (6) while relation (7) extends to [12]:

$$n_{L,R} \cong n \left( 1 \pm \frac{1}{2} \mathbf{Q} \cdot \mathbf{u}_k \right), \quad (9)$$

with  $n$  the complex refractive index, consisting of a real part given by the usual refractive index and an imaginary part given by the absorption coefficient. Accordingly, a complex Faraday rotation is obtained and relation (8) extends to:

$$\theta \cong \frac{\pi L n}{\lambda} \mathbf{Q} \cdot \mathbf{u}_k = \theta_K + i\varepsilon_K, \quad (10)$$

where  $\theta_K$  is the rotation angle and  $\varepsilon_K$  is the ellipticity of the emergent polarized light. As it can be observed from eq.(10) it is enough to know the vectors  $\mathbf{Q}$  and  $\mathbf{u}_k$  (or theirs components), as well as the refractive index and the absorption coefficient of the medium in the absence of the applied field, in order to estimate both  $\theta_K$  and  $\varepsilon_K$ .

The most general macroscopic description of magneto-optics is based on the dielectric tensor theory [13] and principally derives from the Maxwell equations of electromagnetic waves propagating in finite magnetic media and a suitable description of the dielectric tensor according to the Onsager relation which postulate that the symmetry of its off diagonal components under a time reversal is kept only by reversing the magnetic field (or magnetization) [14]. Hence,  $\varepsilon_{ij}(\mathbf{B}) = \varepsilon_{ji}(-\mathbf{B})$  and expanding up to linear terms in  $\mathbf{B}$ , it results (within the assumption that for  $B = 0$  the off diagonal components are zero) that for  $i \neq j$ , each pair of symmetrical components will be proportional to  $\pm$  components of  $\mathbf{B}$ . Therefore, the dielectric tensor is expressed as [10–12]:

$$\tilde{\epsilon} = \epsilon \begin{pmatrix} 1 & iQ_z & -iQ_y \\ -iQ_z & 1 & iQ_x \\ iQ_y & iQ_x & 1 \end{pmatrix}, \quad (9)$$

where  $Q_x$ ,  $Q_y$ ,  $Q_z$  are the components of the Voight vector,  $\mathbf{Q}$  and  $\epsilon$  is the isotropic part of the dielectric constant. There are these diagonal terms, proportional to components of the magnetic field, which modify the light polarization and are responsible for the magneto-optic effects.

### 3. A COMPARATIVE DISCUSSION BETWEEN MOKE AND SQUID MAGNETOMETRY

While most magnetic materials of interest for applications are metals that strongly absorb light, one often proceed to measure magneto optic effects *via* the reflected light and therefore, mainly the magneto optic Kerr effect (MOKE) is used in order to probe the magnetism of metallic surfaces. It is worth mentioning that MOKE is not a pure surface probe, because in case of the metallic surfaces the light penetrates always inside the material over a skin depth of 10–20 nm (evanescent wave) and the change of polarization in the reflected light can be in principle understood also by the Faraday effect (that is also supported by the dependence of the effect magnitude on the film thickness, as soon as thicknesses lower than the skin depths are involved). However, the Kerr effect can be described by a specific macroscopic formalism, based on the fact that the reflection coefficients are dependent on the refractive index of the magnetic film and hence on its dielectric tensor [13, 14]. The general formalism has the advantage that can be extended also to the case of multi-layers [12, 15]. This aspect as well as the latest progress in the development of the experimental techniques makes from MOKE a very powerful and versatile tool for studying magnetic thin films and multi-layers of large technological impact. As compared to conventional magnetometry (counting here also the most performing one based on superconducting quantum interference device, SQUID), MOKE presents a significant number of distinct features: (i) its sensitivity is comparable to the SQUID magnetometry (being able to measure magnetic properties of atomic sub-monolayer thick ferromagnetic samples), in conditions that the set-up is sensible simpler and less expensive, (ii) the data acquisitions is much faster, (iii) ultra-short laser light pulses allows studies on magnetization dynamics (relaxation) on very short time windows, down to fs, whereas intense laser light might induce higher order magneto-optical effects providing additional magnetic information, (iv) the technique can be extended in order to provide element-specific information, especially in case of the X-ray absorption regime, within the magnetic circular and linear dichroism techniques and (v) new versions of MOKE techniques such as vector MOKE and

diffracted MOKE can be developed in order to provide in a much simple manner additional information on magnetic anisotropy or magnetized microstructures which are periodically arranged.

#### 4. A FARADAY CELL BASED MOKE MAGNETOMETER

Depending on the orientation of the magnetization vector with respect to the direction of the incident light, there are three different geometries for the MOKE experiments (see Fig. 2): longitudinal, transverse and polar. In case of the longitudinal geometry, the magnetization is oriented both in the sample plane and in the incidence plane. We illustrate in Fig. 2 the schematics of a longitudinal MOKE, for the case of an incident  $s$ -polarized light. It is to mention that if the electric field of the incoming wave is polarized in the plane of incidence, one deal with a  $p$ -polarized light whereas if it is perpendicularly polarized on the plane of incidence, one deals with a  $s$ -polarized light. For an easier representation, one associates to the above mentioned geometry an orthogonal system, with the  $Oz$  axis along the vector  $\mathbf{k}$ , and the  $Ox$  and  $Oy$  axes along the  $s$ -polarized and  $p$ -polarized components, respectively. When the incident  $s$ -polarized light is reflected off the magnetic surface, a small additional out of phase  $p$ -component appears in the reflected light, due to the oscillating Lorentz force, inducing corresponding oscillations of the electrons. By composing the two out of phase coming electric fields, it results the elliptically polarized light characterized by the rotation of the polarization plane,  $\theta_K$ , and the ellipticity  $\varepsilon_K$  (see relation 10 and Fig. 2). These two parameters have to be experimentally derived in order to monitor the magnetic properties of the bidimensional system and the present literature reports on a large variety of MOKE experimental arrangements providing such information [12].

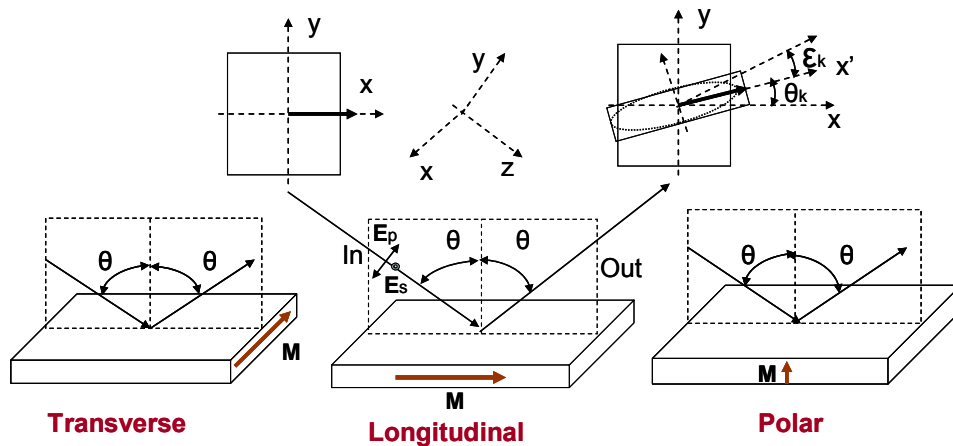


Fig. 2 – A pictorial representation of the three different geometries for the MOKE experiments and a schematic of the polarization states of the light, before and after the reflection on a magnetic film.



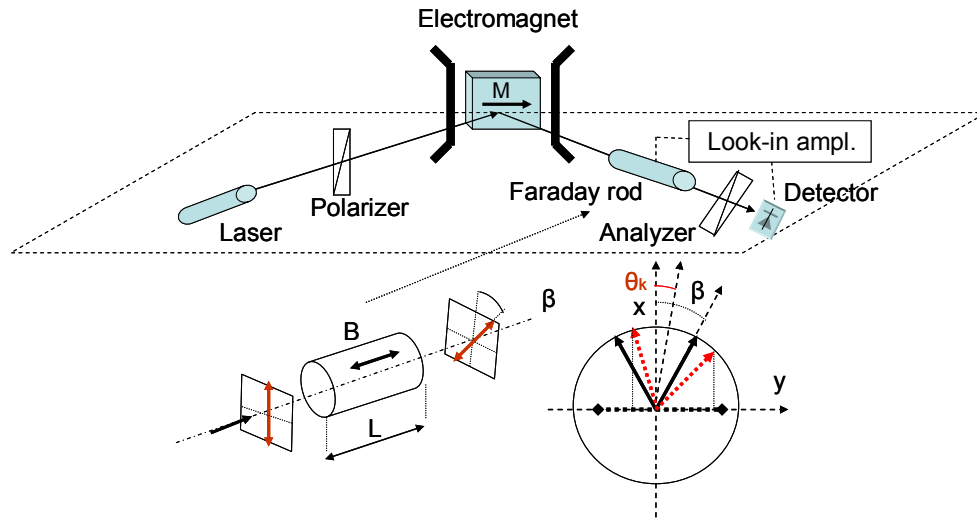


Fig. 3 – A schematic representation of the longitudinal MOKE magnetometer with Faraday cell, for the versatile study of magnetic thin films and multilayers.

A relative simple but very sensitive version based on the detection of the Kerr angle  $\theta_K$  through the detection of the above described  $p$ -component induced by the magnetic surface (Fig. 3) in a longitudinal geometry, will be briefly described in the following. The sensitivity of the method will be finally illustrated *via* some experimental results. The experimental set-up, provided by AMACC, Anderberg & Modeer Accelerator AB, is schemed in Fig. 3. The light emitted by a laser diode ( $\lambda = 635 \text{ nm}$ ), is incident and then reflected at  $45 \text{ deg.}$  *versus* the normal at a magnetized film surface. Initially, it is polarized by a polarizing prism, perpendicular to the incidence plane, in order to select just an  $s$ -polarized component (parallel to the film plane). After reflection, the polarization direction is rotated, depending on the magnetization state of the sample (the magnetic field is applied in the sample plane, along the projection of the  $\mathbf{k}$  vector of the incident light (longitudinal geometry)). After reflection, the light crosses firstly a Faraday cell type modulator, then an analyzer and then reaches a photodiode. The obtained electrical signal is finally amplified by a look-in amplifier which is modulated to the same frequency as the Faraday cell modulator. The key component of the device is the Faraday modulator, of which working principle is also illustrated *via* the inset of Fig. 3. The Faraday modulator consists of a coil with glass core (rod) of length  $L$ , on which can be applied an alternate current of given angular frequency,  $\omega_m$ , *e.g.* commanded by the look-in amplifier. This current generates through the coil an alternate magnetic field of induction  $\mathbf{B}$ . According to the typical Faraday effect, expressed by relation (8), the alternate magnetic field will rotate periodically the polarization direction of the electric field in the reflected light passing through the Faraday rod with an angle  $\beta(t) = K(\lambda)LB_0\cos(\omega_mt) = K^*\cos(\omega_mt)$ . Let's consider the

polarization direction of the light before entering the rod along the axis  $Ox$  (see Fig. 3, right side, down) and the direction of the analyzer along  $Oy$ . The electrical signal at the diode will be proportional to  $I_0 \sin^2 \beta$  and finally proportional to  $I_0 \beta^2$  for enough low angles  $\beta$ , as involved by the Faraday effect. Hence, the alternating electrical signal will present consecutive maxima of equal amplitudes  $A = I_0 K^*$ . If the magnetic field applied on the sample will rotate the polarization direction of the reflected light by the angle  $\theta_K$ , the extreme rotations of the  $\mathbf{E}$  vector after passing through the Faraday rod are  $\beta \pm \theta_K$  (with  $\beta = K^*$ ). Accordingly, the alternating electrical signal will show consecutive maxima of unequal amplitudes, namely  $A_1 = I_0 (K^* + \theta_K)^2$  and  $A_2 = I_0 (K^* - \theta_K)^2$ . It results straightforward within the condition that  $\theta_K \ll K^*$ , the ratio  $R = (A_1 - A_2) / (A_1 + A_2)$  as proportional to  $\theta_K$ . The main advantages of measuring  $\theta_K$  *via* the experimentally obtained  $R$  ratios (averaged over a chosen number of alternations in the detected electrical signal) consists of the simplicity and very high precision of the method and the  $I_0$  independent results, giving rise to the opportunity to compare saturation magnetizations of different samples (evidently, in arbitrary units, due to the proportionality between the Kerr angle and the film magnetization).

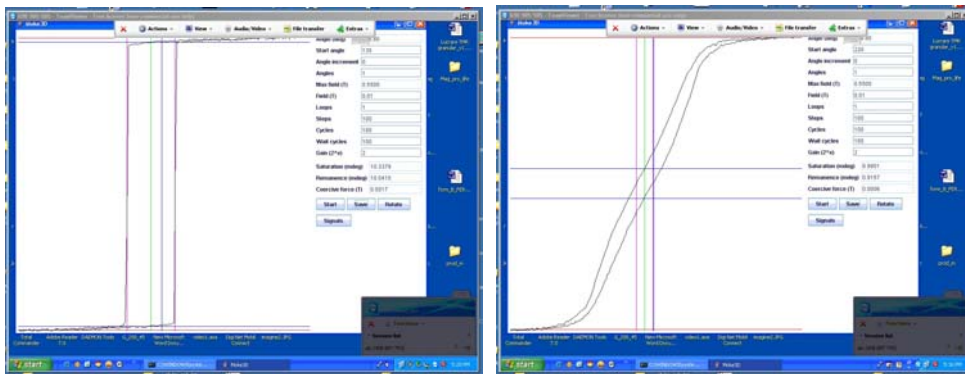


Fig. 4 – Kerr angles *versus* applied fields collected on a 5 nm thick Fe-Co thin film grown on an Ir-Mn underlayer. Two orientations of the field with respect to a reference in-plane direction were considered.

The large capabilities of the method are illustrated *via* the hysteresis loops presented in Fig. 4. The loops, consisting in the dependence of the Kerr angle *versus* an applied magnetic field, have been collected on a 5 nm thick ferromagnetic film of  $\text{Fe}_{50}\text{Co}_{50}$  grown on a 15 nm thick antiferromagnetic  $\text{Ir}_{20}\text{Mn}_{80}$  underlayer on Si(100) substrate, prepared by sputtering in radiofrequency. Two orientations of the magnetic field with respect to the (100) axis of the Si substrate were considered, in order to prove the strong uniaxial anisotropy of the film. The saturation Kerr angle is less than 1 mdeg, in conditions that 0.1 mdeg saturation can be still well resolved. The acquisition of the data can be remotely done by internet, *e.g.* by using the TeamViewer facility.

## 5. CONCLUSIONS

A didactical perspective on the origin of the magneto-optic effects is provided, by starting from the classical idea of the Lorentz force acting on electrons driven by the electric field of the light passing through nonmagnetic or magnetic media, subjected to magnetic fields. The specificity of the MOKE magnetometry with respect to alternative techniques deserving the magnetic characterization of ultrathin films and multi-layers is underlined. The working principles and the performances of a Faraday cell based MOKE magnetometer are presented. The remote control of the device *via* internet makes from it a strong didactical tool for exemplifying high performance characterization techniques of bidimensional nanosystems with technological impact.

*Acknowledgements.* The financial support through the doctoral fellowship by the Project POSDRU 88/I.5/5/56668 is highly acknowledged.

## REFERENCES

1. Keune W, Kuncser V E, Doi M, Askin M, Spies H, Sahoo B, Duman E, Acet M, Jiang J S, Inomata A, and Bader S D, *Mossbauer effect study of the Fe spin structure in exchange-bias and exchange-spring structures*, J Phys: Applied Physics, **35**, 2352 (2002).
2. Radu F and Zabel H., *Exchange Bias Effect of Ferro-Antiferromagnetic Heterostructures*, Springer Tracts in Modern Physics, **227**, 97–184 (2007).
3. Bobo J F, Gabillet L and Bibes M., *Recent advances in nanomagnetism and spin electronics*, J.Phys.C: Condens.Matter, **16**, S471-96 (2004).
- [4] Fert A, George Jean-Marie, Jaffrics H, Mattana R and Senor P., *The new era of spintronics*, Euro.Phys.News, **34**, 6, 10 (2003).
5. Johnson M., *Magnetolectronics*, Elsevier, Amsterdam, 2004.
6. Richter H J and Harkness S D., *Media for Magnetic Recording Beyonds 100 Gbit/in<sup>2</sup>*, MRS Bulletin, 384, 2006.
7. Skomski R and Coey J M D., *Permanent magnetism*, Institute of Physics Publishing Ltd, 1999.
8. Kuncser V E, Doi M, Keune W, Askin M, Spies H, Jiang J S, Inomata A, and Bader S D., *Observation of the Fe spin spiral structure in Fe/Sm-Co exchange spring bilayers by Mossbauer spectroscopy*, Phys. Rev., **B 68**, 064416 (2003).
9. Bostan CG, Dina N, Bulgariu M, Craciun S, Dafinei M, Chitu C, Staicu I, Antohe S, *Teaching/learning photovoltaic effect in high school*, Romanian Reports in Physics, **63**, 2, 543–556, (2011).
10. Davidescu DC, Dafinei M, Dafinei A, Antohe S, *Assessment instrument MERLIN – Metal Resistivity Analysis by Linearization*, Romanian Reports in Physics, **63**, 3, 753–781 (2011).
11. Oppeneer P M., Handbook of Magnetic Materials, Vol. 13, ed by Buschov K.H.J., Elsevier Science 2001.
12. Qiu Z Q and Bader S D., *Surface magneto-optic Kerr effect*, Review of Scientific Instruments, **71**, 3, 1243 (2000).
13. Zak J, Moog E R, Liu C and Bader S D., Phys.Rev., **B 43**, 6423 (1991).
14. Schlenker M and Souche Y., *Les effets magneto-optiques in Magnetisme I*, Fondaments EDP Science 2000.
15. Mansuripur M., *The physical principles of magneto-optical recording*, Cambridge University Press, 1995.